AD-A220 325

UNCLASSIFIED

SECURITY CLASSIFICATION OF THIS PAGE (When Data Entered)

2

## REPORT DOCUMENTATION PAGE

READ INSTRUCTIONS BEFORE COMPLETING FORM

| | |
|---|---|
| 1. REPORT NUMBER: ARO 24623.41-EG-UIR | 2. GOVT ACCESSION NO.: N/A |
| 3. RECIPIENT'S CATALOG NUMBER: N/A | |
| 4. TITLE (and Subtitle): Droplet Sized and Velocities in a Transient Diesel Fuel Spray | 5. TYPE OF REPORT & PERIOD COVERED: Reprint |
| | 6. PERFORMING ORG. REPORT NUMBER: N/A |
| 7. AUTHOR(s): Ja-Ye Koo and Jay K. Martin | 8. CONTRACT OR GRANT NUMBER(s): DAAL03-86-K-0174 |
| 9. PERFORMING ORGANIZATION NAME AND ADDRESS: Univ of Wisconsin, Detroit, Michigan | 10. PROGRAM ELEMENT, PROJECT, TASK AREA & WORK UNIT NUMBERS: N/A |
| 11. CONTROLLING OFFICE NAME AND ADDRESS: U. S. Army Research Office, P. O. Box 12211, Research Triangle Park, NC 27709 | 12. REPORT DATE: 1990 |
| | 13. NUMBER OF PAGES: 19 |
| 14. MONITORING AGENCY NAME & ADDRESS (if different from Controlling Office) | 15. SECURITY CLASS. (of this report): Unclassified |
| | 15a. DECLASSIFICATION/DOWNGRADING SCHEDULE |

16. DISTRIBUTION STATEMENT (of this Report)

Submitted for announcement only.

DTIC ELECTE APR 10 1990 S D

17. DISTRIBUTION STATEMENT (of the abstract entered in Block 20, if different from Report)

18. SUPPLEMENTARY NOTES

The view, opinions, and/or findings contained in this report are those of the author(s) and should not be construed as an official Department of the Army position, policy, or decision, unless so designated by other documentation.

19. KEY WORDS (Continue on reverse side if necessary and identify by block number)

20. ABSTRACT (Continue on reverse side if necessary and identify by block number)

ABSTRACT ON REPRINT

DD FORM 1 JAN 73 1473 EDITION OF 1 NOV 65 IS OBSOLETE

UNCLASSIFIED

SECURITY CLASSIFICATION OF THIS PAGE (When Data Entered)

SAE The Engineering Society For Advancing Mobility Land Sea Air and Space®
INTERNATIONAL

400 COMMONWEALTH DRIVE, WARRENDALE, PA 15096-0001 U.S.A.

# SAE Technical Paper Series

900397

# Droplet Sizes and Velocities in a Transient Diesel Fuel Spray

**Ja-Ye Koo and Jay K. Martin**
University of Wisconsin-Madison
Engine Research Center



**International Congress and Exposition**
**Detroit, Michigan**
**February 26 — March 2, 1990**


*All SAE papers are abstracted and indexed in the SAE Global Mobility Database.*



**ISSN 0148-7191**


Positions and opinions advanced in this paper are those of the author(s) and not necessarily those of SAE. The author is solely responsible for the content of the paper. A process is available by which discussions will be printed with the paper if it is published in SAE Transactions. For permission to publish this paper in full or in part, contact the SAE Publications Division.

Persons wishing to submit papers to be considered for presentation or publication through SAE should send the manuscript or a 300 word abstract of a proposed manuscript to: Secretary, Engineering Activity Board, SAE.

**Printed in USA**

900397

# Droplet Sizes and Velocities in a Transient Diesel Fuel Spray

**Ja-Ye Koo and Jay K. Martin**
University of Wisconsin-Madison
Engine Research Center

ABSTRACT - Simultaneous droplet sizes and velocities were obtained for a transient diesel fuel spray in a quiescent chamber at atmospheric temperature and pressure. Instantaneous injection pressure, needle lift, and rate of injection were also measured, allowing calculation of the instantaneous nozzle discharge coefficient. Short-exposure still photographs were obtained at various chamber pressure and densities to further investigate this spray.

Correlations between droplet size and velocity were determined at each crank angle to observe the detailed nature of the transient events occurring in this transient diesel fuel spray. As expected, peak mean and rms velocities are observed in the center of the spray. Measured average velocities are consistent with a calculated value, using the discharge coefficient for the nozzle and the known rate of fuel injection. The spray was nearly symmetric, with higher velocities occurring near the injector tip, and the radial dependence of velocity consistent with that observed from the spray photographs. Factors observed to effect the droplet size and velocity distributions and history include pump speed, fuel quantity delivered, and needle lift.

The measured droplet diameters range in size from approximately the same size as the nozzle diameter to micron-sized droplets. The size distributions tend to have expected shapes, with a very strong dependence on time and position in the spray.

The spray photographs taken at low ambient pressure conditions reveal the existence and characteristic frequency of surface waves on the liquid exiting from the nozzle. These waves are less obvious at atmospheric pressures, and completely obscured by aerodynamic effects on the spray structure at chamber densities typical of that encountered in diesel injection.

INTRODUCTION - The distribution of fuel in the combustion chamber of direct-injection engines is a dominate factor in determining the characteristics of the combustion process. Unfortunately, the fuel injection process that, in part determines this fuel distribution is not well understood. The physical parameters which influence the fuel spray include fuel properties, the system for producing high pressure fuel at the nozzle, the injection nozzle itself, the combustion chamber geometry, the hydrodynamics, and the operating condition [1]*. There have been many experimental [2-13] and theoretical [14-19] studies of fuel sprays, to reference just a few. Most of these experiments have been carried out under steady, or non-engine like conditions. There remains a need for detailed information about droplet size and velocity distributions for transient diesel sprays [20]. Knowledge of droplet sizes and velocities should help in the understanding of the structure of the spray, as well as providing the foundation for validation of theories and computational models of sprays. The ultimate objective of spray research is to be able to understand and predict the behavior of transient fuel sprays at engine-like conditions. For this study we report on a step toward that objective, as the data provided here should be useful in the validation of models of spray behavior, as well as providing an indication of the physical structure of these sprays, in terms of droplet sizes and velocities.

---

* Numbers in brackets designate references listed at the end of the paper.

EXPERIMENTAL APPARATUS AND TEST MATRIX - The primary diagnostic used in this study for the measurement of droplet sizes and velocities is an Aerometrics Phase Doppler/Particle Analyzer (PDPA). The PDPA is an extension of the classical dual-beam Laser Doppler Velocimeter (LDV) with three detectors in the receiving optics for the determination of droplet or particle diameter. The instrument has been tested for the validity of its application to sprays [21-26]. In short, this instrument has been demonstrated to accurately provide fundamental data in relatively non-dense sprays. Dense sprays, such as the one investigated here, require much care in the use of the instrument. Because of practical limitations of the instrument and the complex nature and density of these sprays, it is unlikely that the accurate measurement of flux quantities can be accomplished. However, statistical quantities, such as the Sauter Mean Diameter (d32), are very likely representative of the spray, if the instrument is used correctly. The data presented here represent the results of many variations in instrument operation, such as PMT voltage, frequency shift, and optical configuration, to ensure that the results were repeatable and consistent, and physically realistic. For example, velocity only measurements produced droplet velocity distributions that were very similar to the droplet velocity distributions obtained when simultaneous drop sizes and velocities were measured. With velocity only, the measured data rejection ratio was less than 1 % throughout the spray. When velocity and size were measured simultaneously, the validation ratio near the nozzle tip was as small as 20 % due to non-spherical droplets or multiple droplets in the measurement volume. It is possible that the results may not represent the ensemble actually occurring in the spray, although the consistency achieved in the results measured over a wide range of instrument settings makes this unlikely.

All the data to be reported were obtained with the measurement position fixed relative to the injector tip, not relative to the spray. The spray itself shows some variation in position of the edge of the spray from one spray to the next, which may effect the distributions, although photographs of the spray demonstrate these variations to be small.

Figure 1 shows a schematic of the experimental arrangement where the x-axis is coincident with the central axis of the injector, and r is perpendicular to the central axis of the transmitter. With the system shown in Fig. 1, the pump can be operated continuously, with com-

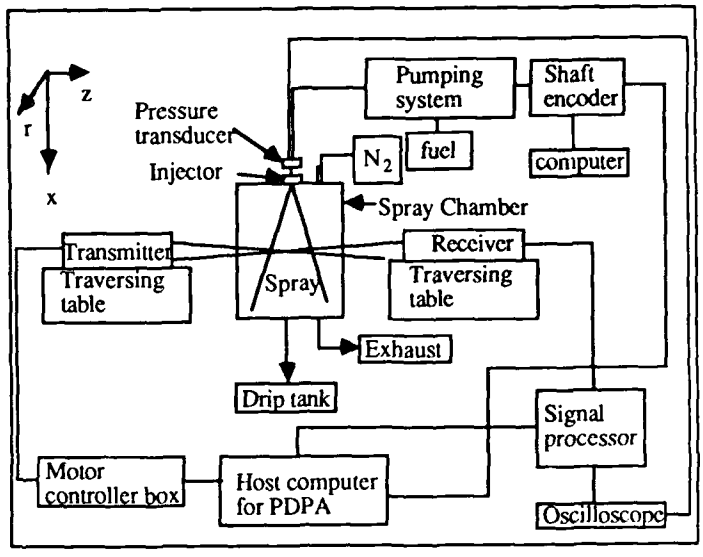


Fig 1. Schematic diagram of experimental apparatus.

**Table 1** Experimental matrix and conditions

| pump speed (rpm) | fuel delivery (mg/Inj.) | chamber pressure |
|---|---|---|
| 400 | 9.5<br>19.0<br>41.5 | Atmospheric pressure |
| 800 | 10.7 | Atmospheric pressure |
| | 19.5 | Atmospheric pressure<br>4 mm Hg<br>1.34 MPa |
| | 40.7 | Atmospheric pressure |
| 1200 | 10.5<br>19.7<br>39.1 | Atmospheric pressure |

Chamber temperature; room temperature
Nozzle; Lucas-CAV single hole
Hole length: 0.8 mm
Hole diameter: 0.406 mm
Static opening pressure: 13.89 MPa
Fuel; Phillips No. 2D Diesel fuel
Refractive index: 1.4748
*Data of droplet size and velocity were taken at atmospheric pressure and three different rpm and fuel delivery.
*Photographs were taken at 800 rpm, 19.5 mg per injection and three different pressures.

puter-controlled selection of the specific injections that will occur in the test chamber. This allows for purging of the chamber between injections, for example. Details of the spray chamber, and the spray photography are included in Ref. [17].

A critical issue in these dense sprays, where there exists large gradients in velocity and droplet size distributions, is the size of the measurement volume. Because of the requirement to have measurements of the Doppler burst phase shift between at least two different positions in the scattered light fringe pattern, the aperture in the receiving optics is rectangular rather than the more typical circular geometry. The width of the aperture used in this set of measurements was 50 μm, which produces an effective measurement volume width of 103.1 μm. For the most frequently used optical configuration (300 mm transmitting lens, 160 mm collimating lens), the measurement volume diameter was approximately 200 μm. An estimate of the observed measurement volume length is approximately 552 μm. To reduce the effects of spatial averaging that could occur, particularly for the measurements made along the radial coordinate, the measurement volume was moved normal to the transmitter axis.

The experimental matrix followed is listed in Table 1. A range of pump speeds and fuel quantity injected are included to observe these effects on the spray behavior. In addition to the injector characteristics listed in Table 1, this injector is instrumented with a Hall-effect transducer for the measurement of needle lift, and a set of strain gages oriented to measure hoop strain in the injector barrel. The output of the strain gages can be calibrated to provide a measurement of instantaneous tip pressure. The fuel used was a Phillips 2D diesel fuel. The measurement of droplet size with the PDPA depends on an accurate refractive index; the fuel used here was specified in separate tests as shown in Table 1.

RESULTS - Presented first are results from characterization of the performance of the nozzle and injection system. Shown in Fig. 2 are the crank-angle resolved tip pressure, needle lift, rate of injection, and discharge coefficient for this experimental pump/injector system for a range of fuel delivery rates.

The rate-of-injection measurements were obtained with a Bosch-type rate-of-injection meter built at the ERC. The output of this instrument is a measure of the relative rate-of-injection during the injection event. To produce a quantitative result, the instantaneous rate-of-injection was integrated over the injection duration and normalized to produce a total quantity of fuel delivered equal to that obtained from direct measurement of the average fuel delivered per injection. Further detail of the rate-of-injection measurement can be found in Ref. [27].

The discharge coefficient was determined from the tip pressure and rate-of-injection measurements according to

$$C_d = \frac{\dot{m}_{actual}}{\rho A \sqrt{2\Delta P/\rho}} \qquad (1)$$

As shown, the rate-of-injection and discharge coefficient rise rapidly as the needle opens to relatively constant values of 3.5 mg/cam degree and 0.72, respectively. The rate of change in these quantities is much greater during nozzle opening than during nozzle closing, which will be evident in the velocity/size data that will be shown. Because this particular arrangement of pump and injector were used in conditions from near vacuum (4 mm Hg) to ambient densities typical of that observed in engines, the retraction valve in the pump was optimized to give the best performance (fewest afterinjections) over the range of conditions studied. In the case of the highest fuel delivery, there is a small afterinjection, which will also be observable in the velocity/size data.

To show the characteristics of the distribution of the velocity/diameter data, the data actually acquired are plotted, along with the Sauter Mean Diameter, d32, defined

$$\bar{d}_{32}(\bar{\theta}, \Delta\theta) = \frac{\sum_{i=1}^{N_c}\sum_{j=1}^{N_i} d_{ij}^{\,3}(\bar{\theta} \pm \frac{\Delta\theta}{2})}{\sum_{i=1}^{N_c}\sum_{j=1}^{N_i} d_{ij}^{\,2}(\bar{\theta} \pm \frac{\Delta\theta}{2})} \qquad (2)$$

an ensemble average of the velocity, U, defined

$$\bar{U}(\bar{\theta}, \Delta\theta) = \frac{1}{N_t}\sum_{i=1}^{N_c}\sum_{j=1}^{N_i} U_{ij}(\bar{\theta} \pm \frac{\Delta\theta}{2}) \qquad (3)$$

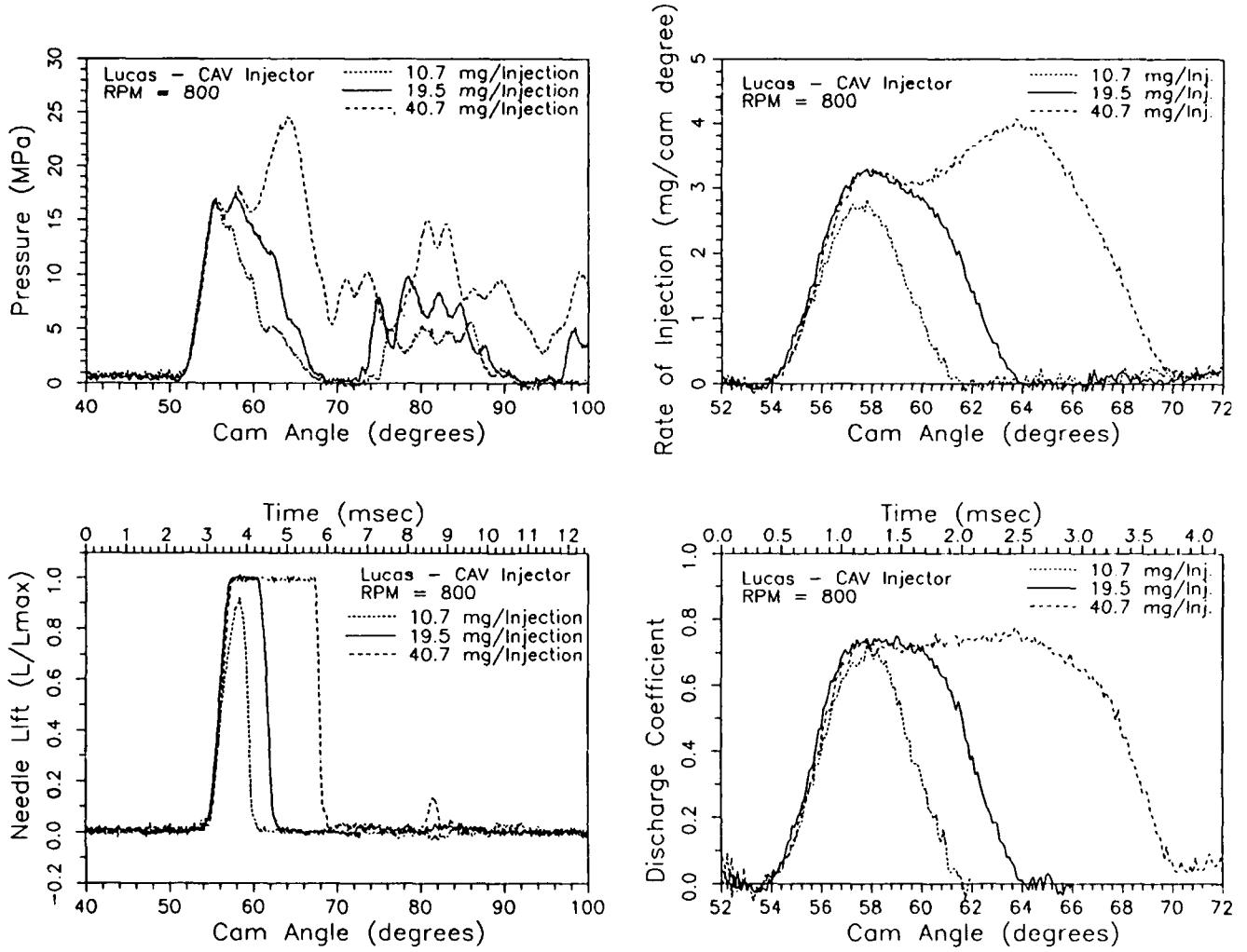


Fig 2. Crank-angle resolved tip pressure (a), needle lift (b), rate of injection (c), and discharge coefficient (d) for three different fuel quantities.

and an rms velocity, Urms, defined

$$U_{rms}(\bar{\theta}, \Delta\theta) = \left[\frac{1}{N_t}\sum_{i=1}^{N_c}\sum_{j=1}^{N_i} u_{ij}^2\left(\bar{\theta} \pm \frac{\Delta\theta}{2}\right)\right]^{\frac{1}{2}} \qquad (4)$$

where $u_{ij} = U_{ij} - U$

Each of these quantities are crank-angle dependent. The actual data acquired are displayed to illustrate the characteristics of the velocity and size distributions, which are not evident from the single statistical parameters of d32 and U.

It should be emphasized that because of the large range of diameters observed in the data (from the order of a micron to the nozzle hole diameter), and the limitation on droplet size range (35:1), the PDPA could not cover the range of droplet sizes at one instrument setting. Thus the data presented are the data that were obtained at one unique instrument setting. For the case of the axial variations to be presented, d32 should be representative of the ensemble, although extreme concentrations of very small drops (less than 8.6 microns in diameter) could reduce the numbers obtained. For the radial variations, in order to capture the large number of small drops occurring on the periphery of the spray, a smaller size range was used. In this case, d32 is not characteristic of the spray near the centerline, since droplets outside this range occur there. However, this does not invalidate the trends observed here or eliminate the use of this data for model validation. To compare this data with model results, one would

calculate with no limits on droplet size, and extract results with a size range identical to that used in the measurements. The results should then be comparable.

Velocity/Diameter Results - First, the axial dependence of the velocity and diameter are considered for a single operating condition which is characteristic of the behavior of the system. Results from four different locations along the axis of the spray are shown in Fig. 3. For all of the velocity/size results to be presented, 2000 data samples were obtained in 50 to 100 injections. The velocity and size are plotted crank-angle resolved, such that the transient nature of the spray can be observed. A calculated average discharge velocity calculated from the measured pressure and discharge coefficient shown in Fig. 2 is 147 m/sec. From Fig. 3(a) and 3(b), 1) the peak velocities are reduced as the axial distance from the nozzle is increased, 2) close to the nozzle, the first injected droplets are apparently quickly overtaken by the droplets that follow them, 3) the rate at which the velocity drops after the end of injection is reduced as the axial distance from the nozzle is increased, 4) the droplet diameter range is much larger nearer the nozzle, giving much larger values of the d32 near the nozzle, 5) the distributions of droplet size do not appear to be unusual, and 6) two fairly distinct velocity/diameter groups near the nozzle, with high velocities occurring for the complete range of sizes, and low velocities occurring for mostly small droplets. This, of course, corresponds to the observed wide droplet diameter range during injection, that quickly changes to mostly small droplets at the end of injection. This is demonstrated in Fig. 4, where the velocity/diameter correlations at 10 mm from the nozzle have been separated into one crank-angle degree windows. Figure 5 has the same type of data, in this case for an axial position 30 mm from the nozzle. The trends at this position appear to be similar, although there is a higher concentration of small droplets, as might be expected from droplet breakup.

The effects of fuel quantity injected are shown in Fig. 6. As the fuel quantity is increased, the amount of time that the injection displays steady behavior increases. At highest fuel delivery rate, the highest velocities occur at the point where steady behavior ends. Note that at this point the data density is less than that of other times during the injection. The afterinjection observed in Fig. 2 is clearly visible in the velocity history. This phenomenon does not appear to be influencing the main injection event in any way. Further, it is interesting to note that the afterinjection does not contain any large droplets. Figure 1 shows that the needle barely opens during this injection, which perhaps limits the diameter of the droplets to less than 50 microns.

Pump rotational speed has a strong effect on the behavior of the spray, as shown in Fig. 7. For this injection system, the maximum velocity of the droplets was reduced at the 400 rpm speed, but similar at the higher speeds. Comparisons of the observed velocities with that predicted by the tip pressure and nozzle discharge coefficients showed similar results. At 1200 rpm, the data density during the beginning and middle portions of the injection is less than what it is at the lower pump speeds. This is probably due to the greater penetration of larger non-spherical droplets, or ligaments from the higher pump speed. Note that at the 400 rpm condition, the behavior of the spray is never steady, as the velocity and droplet size distribution change throughout the duration of the spray.

Both drop velocity and diameter distributions show very strong dependence on the radial position in the spray. This is demonstrated in Figure 8(a) and 8(b). For this data the size range of the instrument was changed, because of the large numbers of very small droplets found on the edges of the spray. In order to directly compare the results, the data was obtained with a single size range which would capture these small droplets. A physical picture of the structure of the spray can be formed from Fig. 8(a) and 8 (b); at 30 mm from the spray nozzle, the spray is approximately 8 mm in radius for a very short time period immediately after the start of injection. This indicates that the spray angle is largest just after needle opening. This phenomena was also identified in the short-exposure still photographs. The data density obtained in beginning and middle of the spray, for example between 57 degrees and 65 degrees in Fig. 8 (a), increases with radial distance. This likely indicates that along the spray axis, there are many irregularly-shaped large droplets or ligaments which reduces the data density. Note that the measurement position (30 mm from the nozzle) is within a measured break-up length (50 mm) for similar conditions [4]. The droplets at the edge of the spray are almost all small droplets (d32 less than 20 microns). The largest droplets and peak velocities occur right on the axis of the spray. There is a continuous decrease in the magnitude of these quantities and the

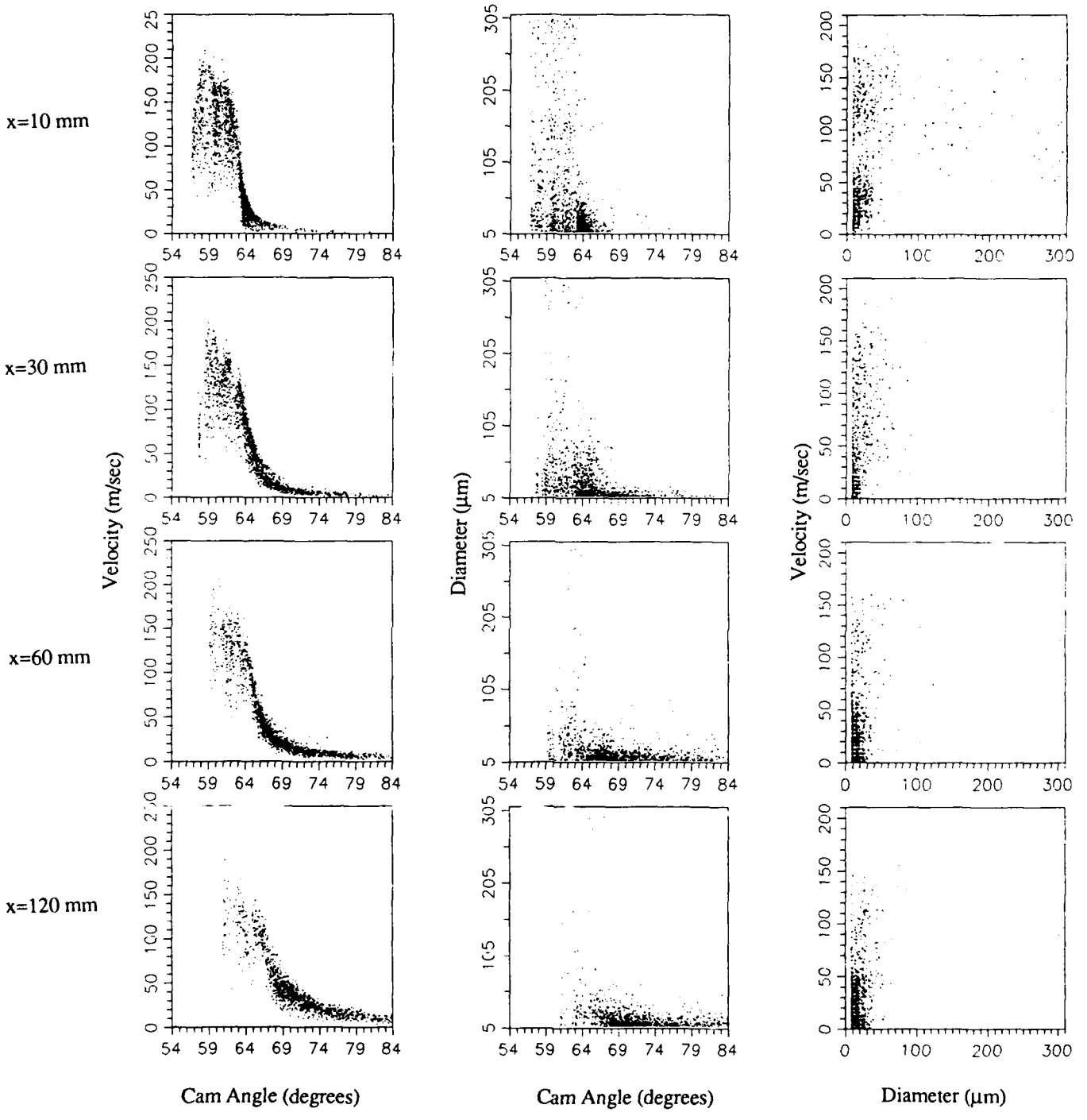


Fig 3(a). Crank-angle resolved axial droplet velocities, sizes, and its correlations at 800 rpm, 19.5 mg per injection, and chamber pressure equal to 1 atm. P/DPA instrument settings: Size range; 8.6 - 300 μm, Velocity range; 0.73-207 m/sec.

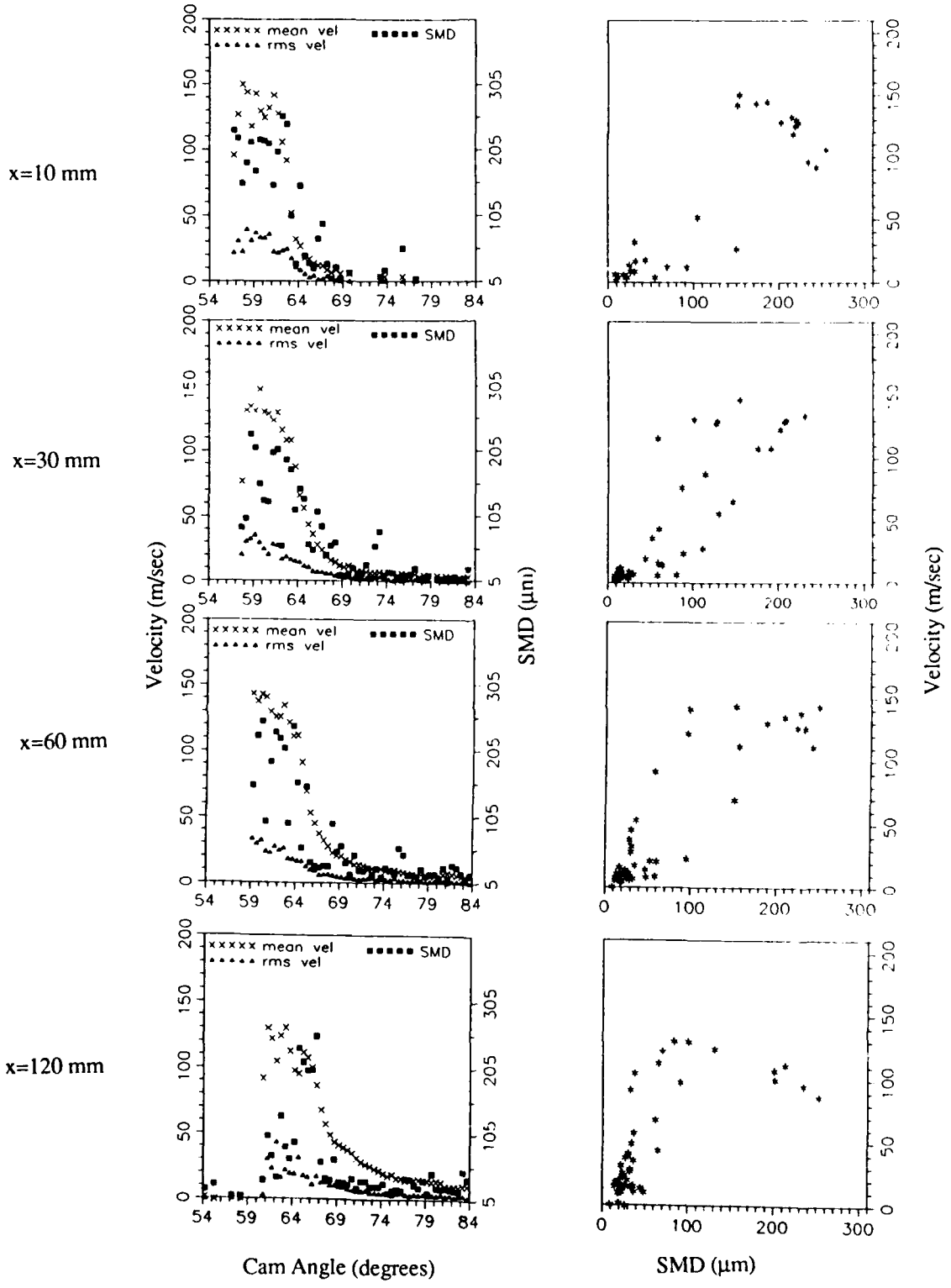


Fig 3(b). Crank-angle resolved SMD, mean velocities, RMS velocities, and its correlation along spray axis.
Each data was ensemble averaged from 50 injections with 0.5 degree resolution. Other conditions are same as Fig 3(a).

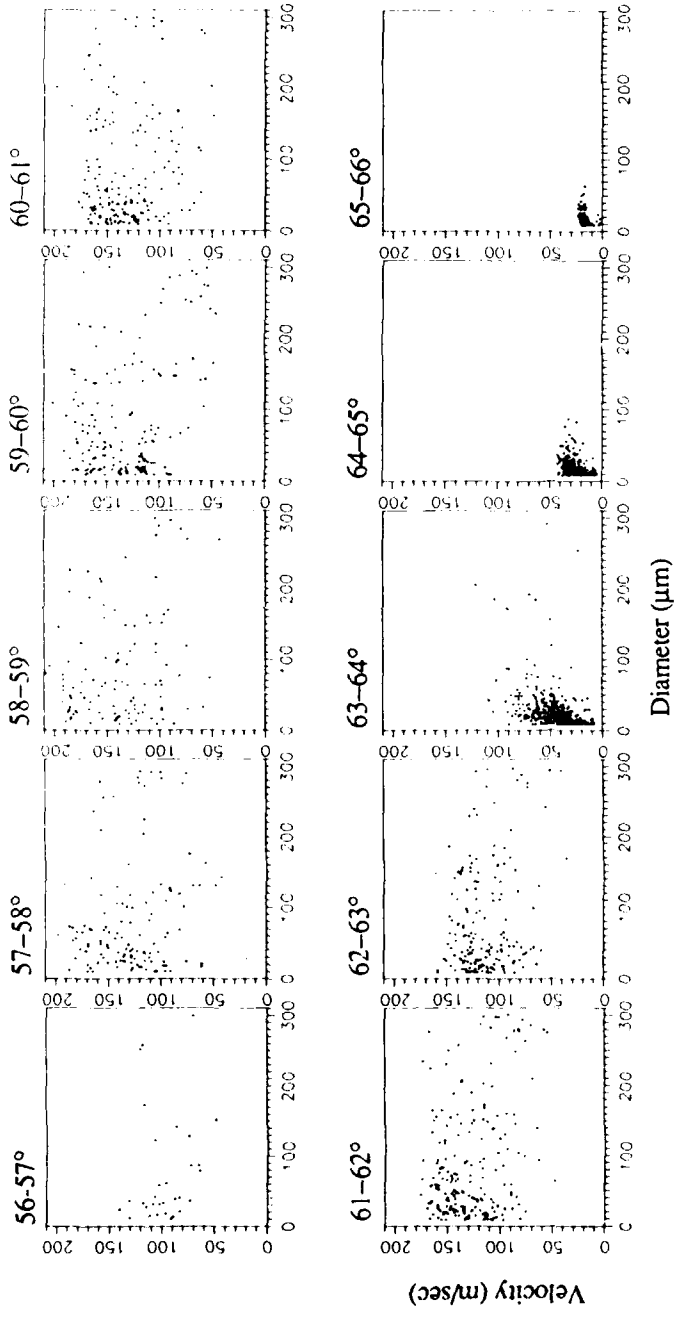


Fig 4. Correlations between droplet sizes and velocities for each cam crank angle at a pump speed of 800 rpm, 8.5 mg per injection, and chamber pressure equal to 1 atm. The measurement volume was located on the axis of the spray 10 mm from the nozzle tip. P/DPA instrument settings: Size range; 8.6 - 300 µm, Velocity range; 0.73 - 207 m/sec.

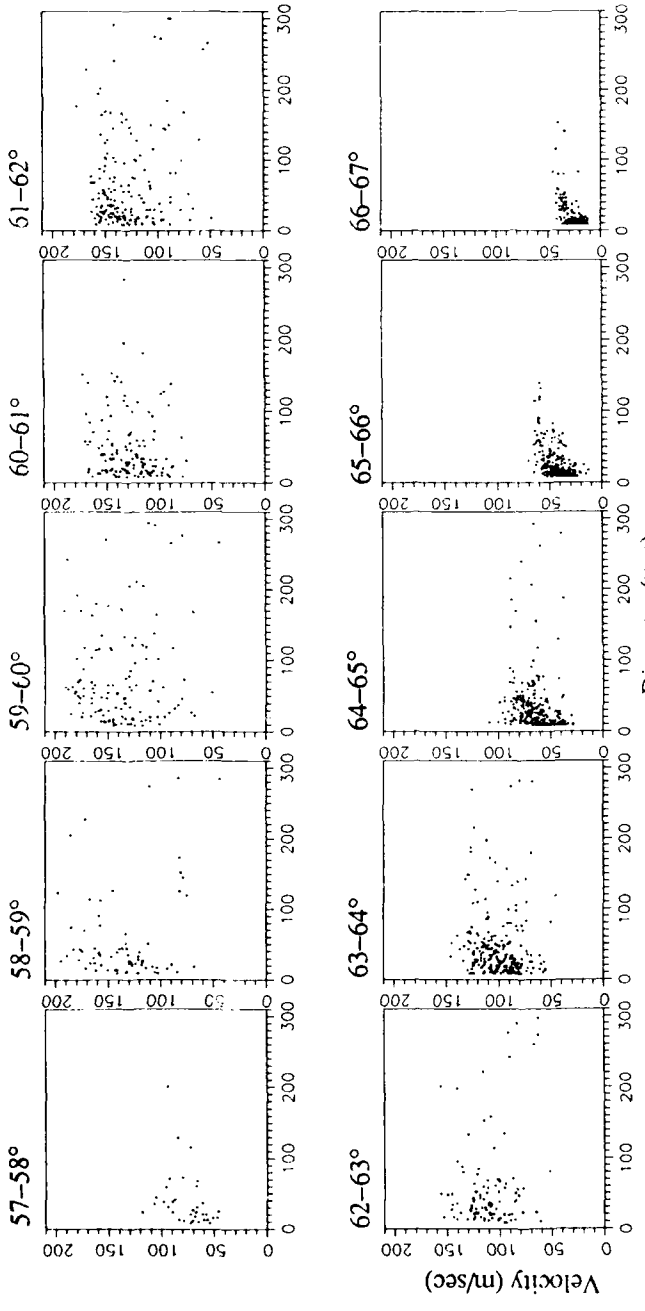


Fig 5. Correlations between droplet sizes and velocities for each cam crank angle at a pump speed of 800 rpm, 8.5 mg per injection, and chamber pressure equal to 1 atm. The measurement volume was located on the axis of the spray 30 mm from the nozzle tip. P/DPA instrument settings: Size range; 8.6 - 300 µm, Velocity range; 0.73 - 207 m/sec.

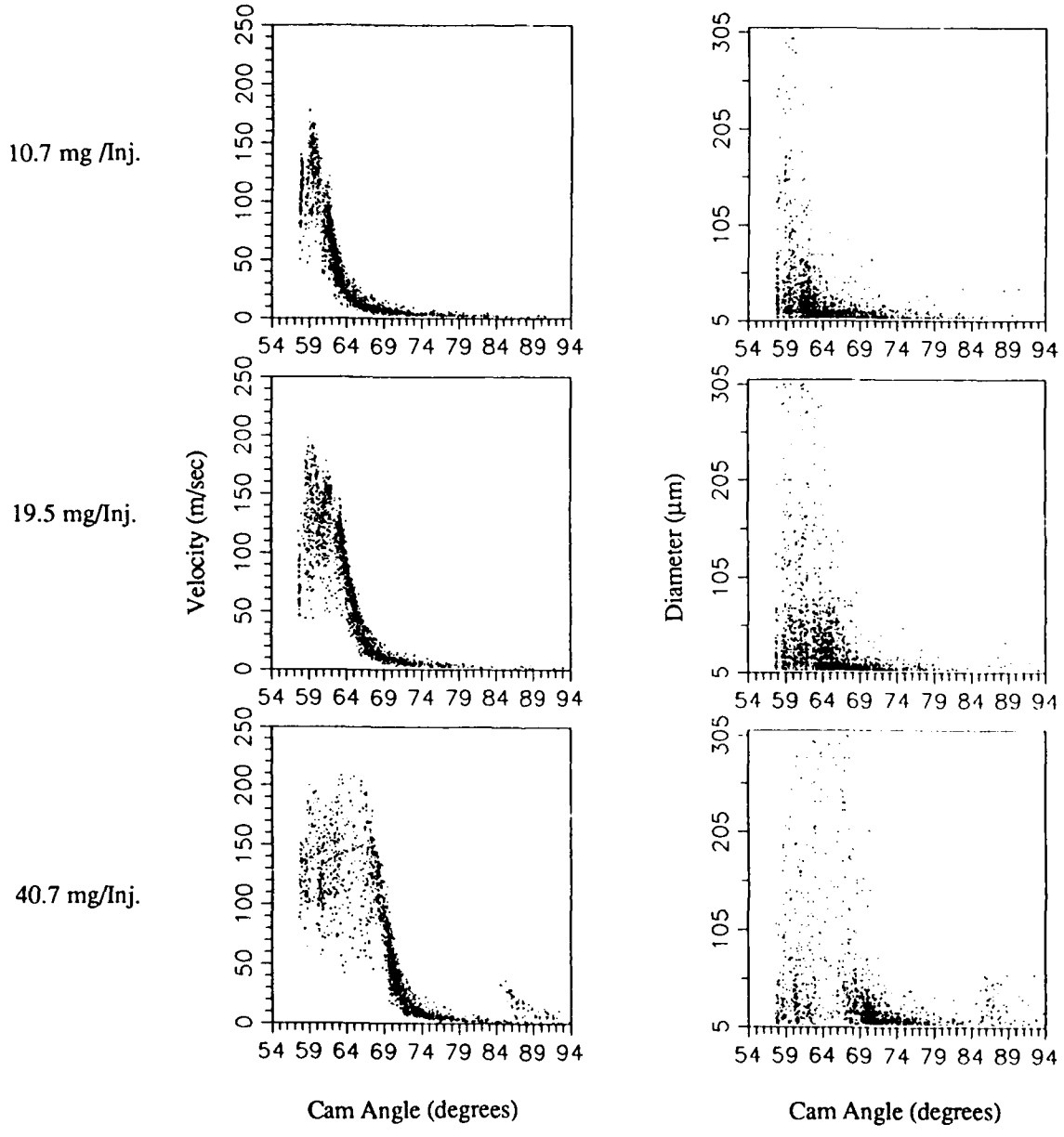


Fig 6. Crank-angle resolved droplet velocity and size distribution for different fuel quantities at 800 rpm. The measurement volume was located on the axis of the spray 30 mm from the nozzle tip. P/DPA instrument settings: Size range; 8.6 - 300 µm, Velocity range; 0.73 - 207 m/sec.

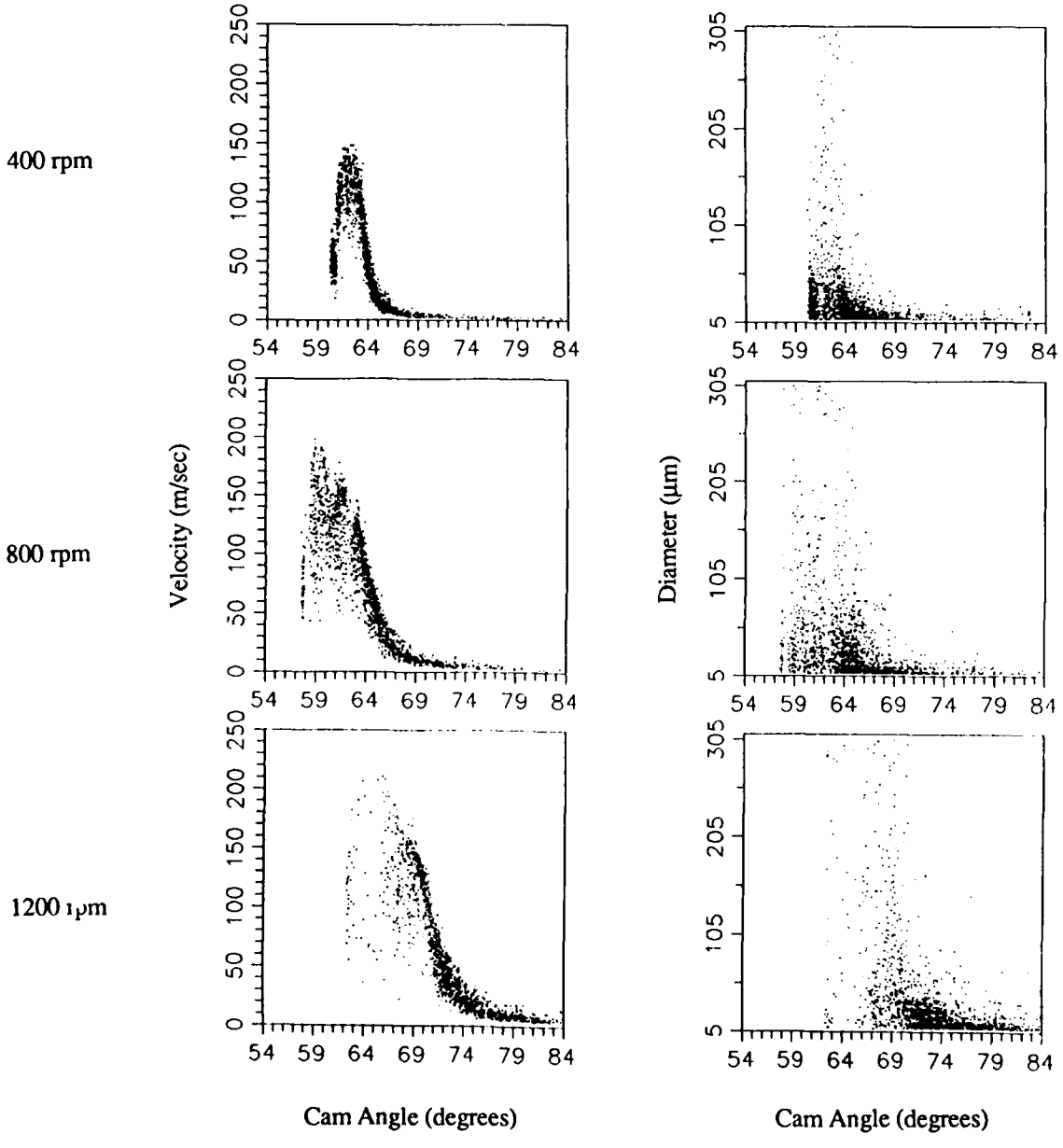


Fig 7. Crank-angle resolved droplet velocity and size distribution for different pump speeds at about 20 mg per injection. The measurement volume was located on the axis of the spray 30 mm from the nozzle tip. P/DPA instrument settings: Size range; 8.6 - 300 µm, Velocity range; 0.73 - 207 m/sec.

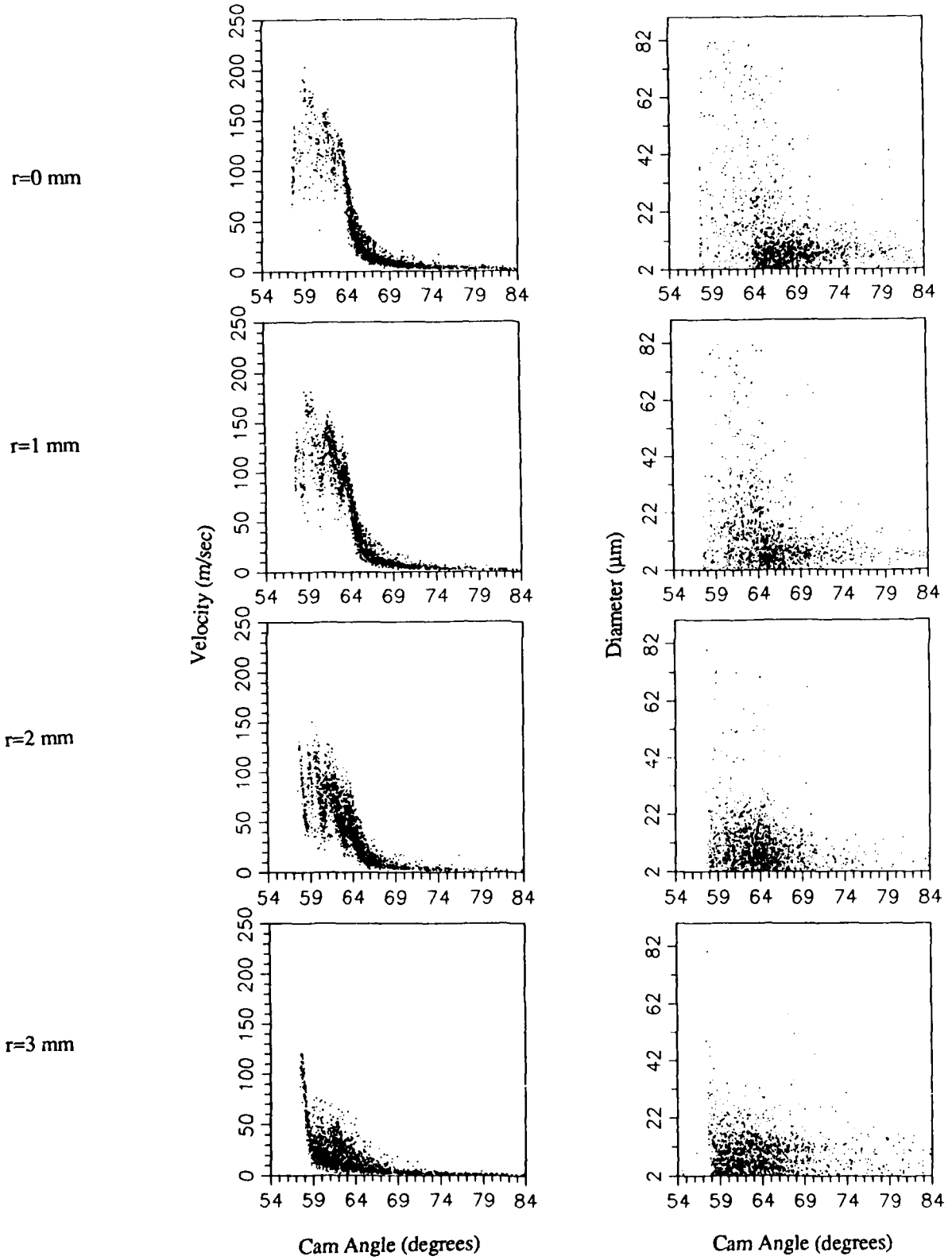


Fig 8(a). Crank-angle resolved droplet velocities, sizes along radial positions at 30 mm from nozzle tip in condition of 800 rpm, 19.5 mg per injection, and atmospheric chamber pressure. P/DPA instrument settings: Size range; 2.3 - 80 µm, Velocity range; -3.0 - 200 m/sec.

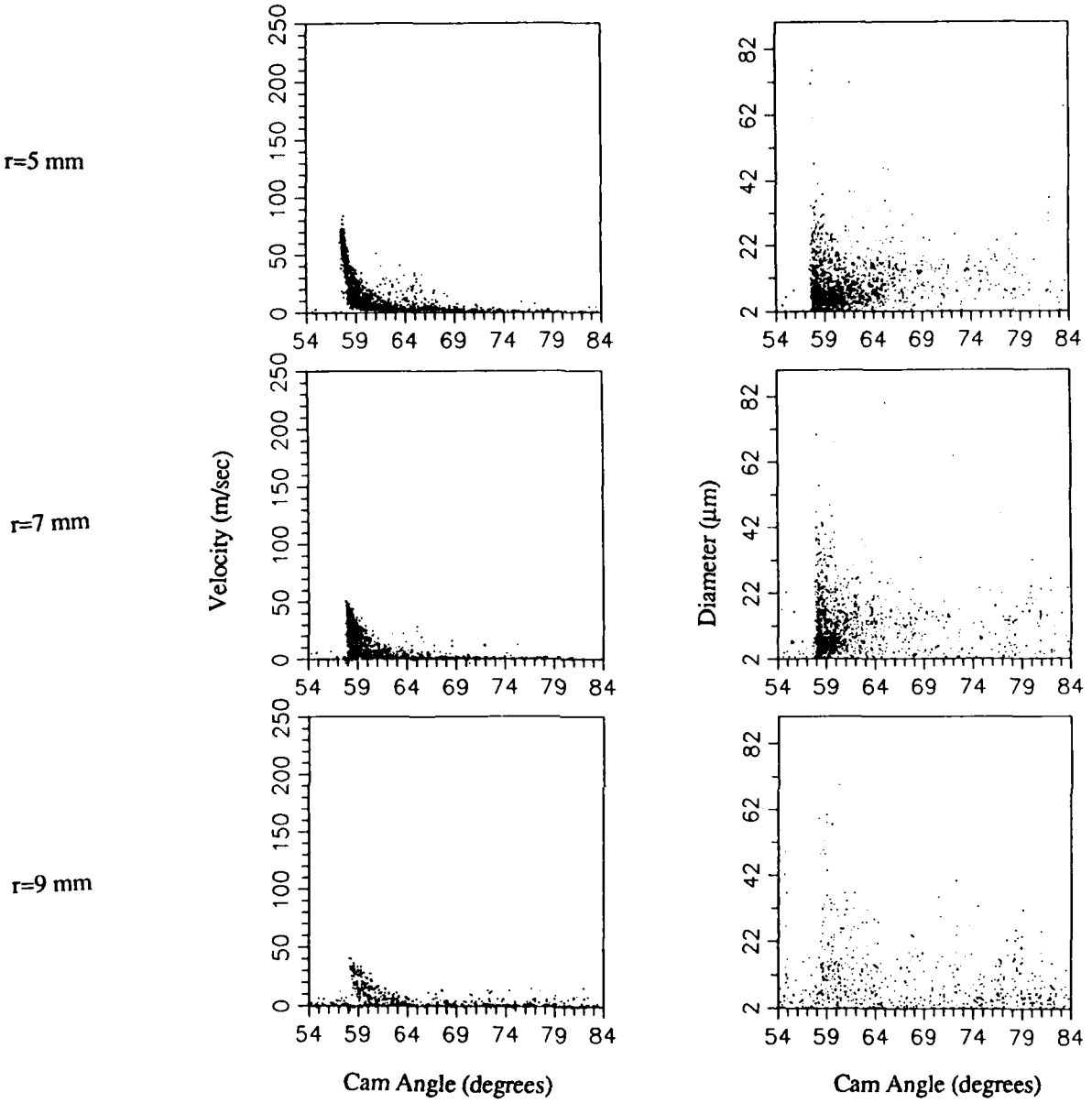


Fig 8(a) continued

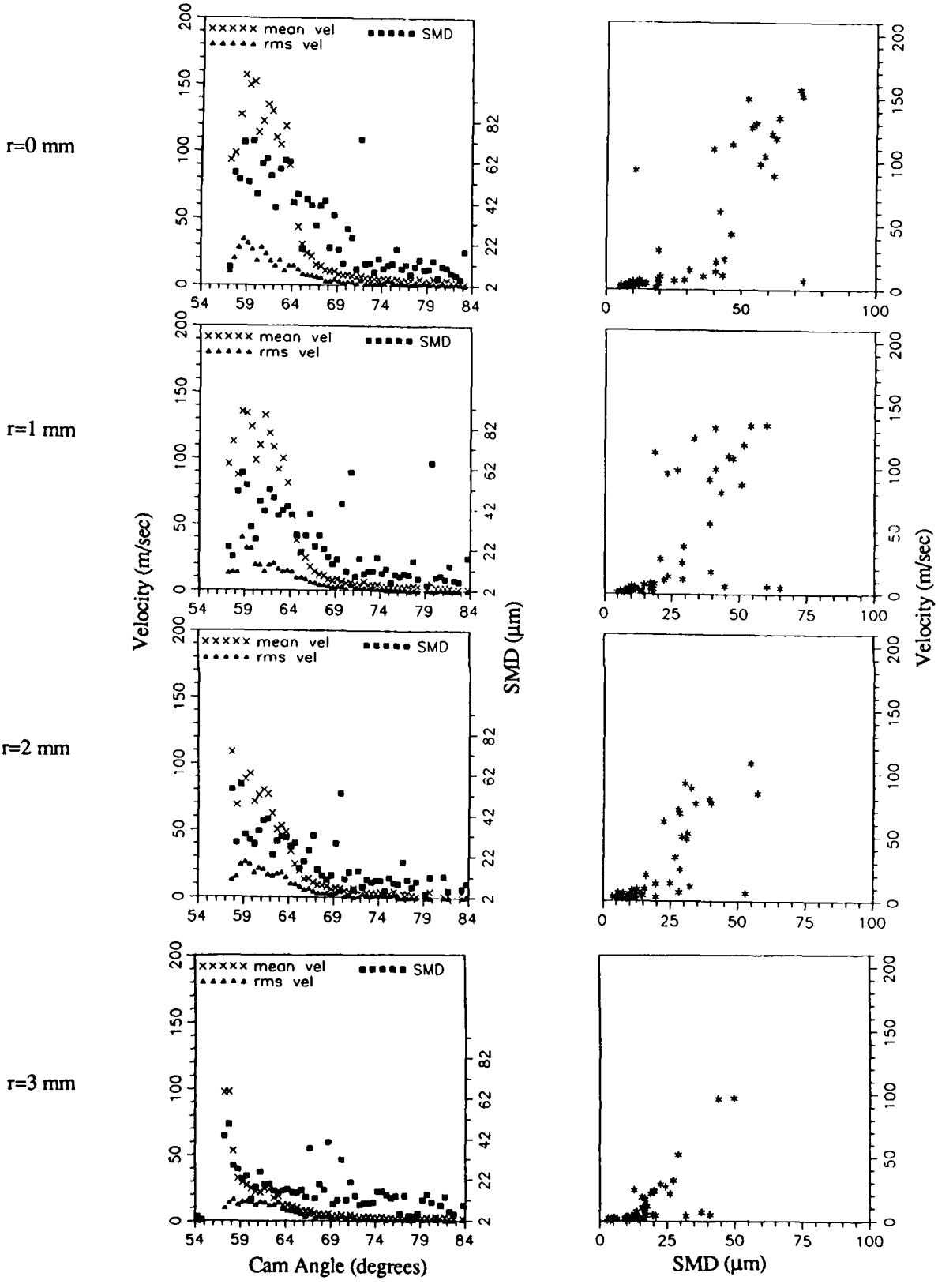


Fig 8(b). Crank-angle resolved SMD, mean velocities, RMS velocities, and its correlation along radial positions at 30 mm from nozzle tip. Each data was ensemble averaged from 50 injections with 0.5 degree resolution. Other conditions are same as Fig 8(a).

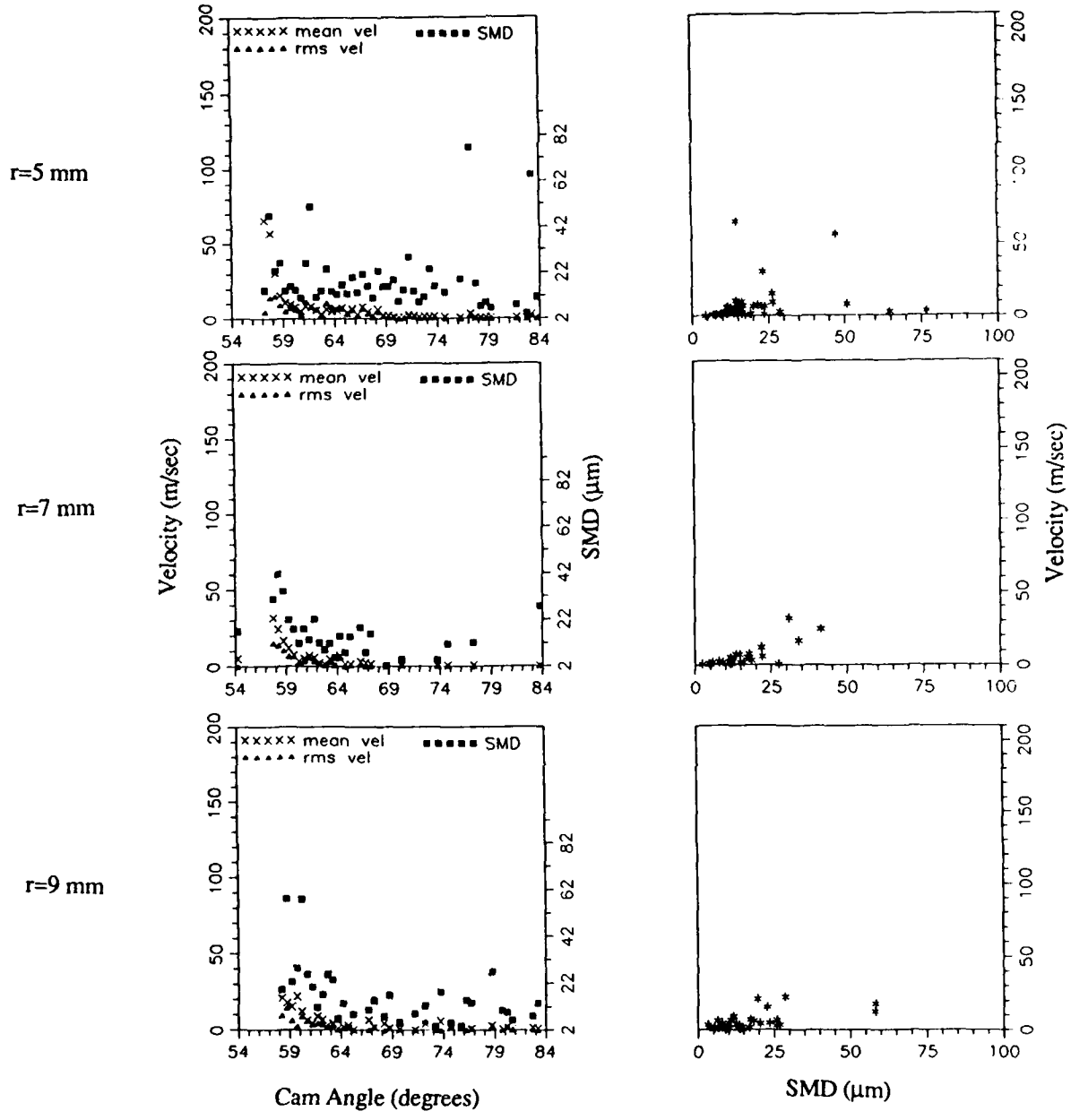


Fig 8(b) continued

time at which they are affected by the transient injection as the radial coordinate is increased.

An estimated droplet relaxation time for a 5 micron droplet to decelerate to 97 % of the gas-phase velocity (assumed to be stagnant) is 60 μs in a distance of 9 mm. Thus, using velocities obtained from droplets 5 microns in diameter and smaller, gas-phase velocities are shown in Fig. 9. Ten mm from the injector tip, the gas velocity achieves velocities of 150 m/s immediately after the start of injection. Just as rapidly, the gas phase velocity falls to zero as injection ends. At 30 mm from the injector tip, the peak velocities are actually increased. However, farther from the nozzle, the peak velocities experienced by the gas are reduced, and the time which the entrained gas decelerates is much longer.

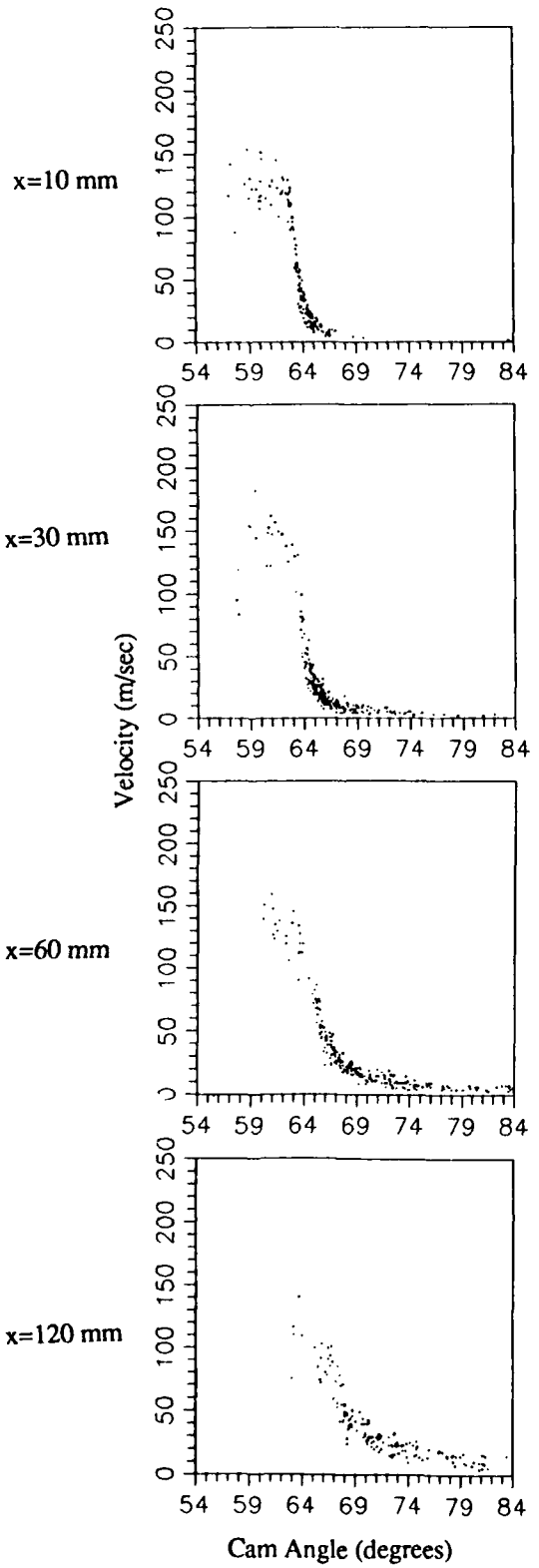


Fig 9. Gas phase axial velocity along spray axis at 800 rpm and 19.5 mg/Injection. Droplet whose size is less than 5 μm assumed to follow gas phase velocities. P/DPA instrument settings: Size range; 2.3 - 80 μm, Velocity range; -3.0 - 200 m/sec.

Short-Exposure Still Photographs - To understand more about the structure of the spray in which these measurements were obtained, the spray was photographed with a very-short exposure (10-60 ns) produced by a copper-vapor laser. Several of these photographs are shown in Fig. 10. Three different chamber conditions were used, air at 4 mm Hg pressure and room temperature, air at atmospheric pressure and room temperature, and N2 at 1.34 MPa and room temperature. As one would expect, the rate of penetration decreases with ambient density, which increases the spread angle of the spray. The average spray tip velocity between 56 CA and 57.4 CA, as estimated from the photographs was 124 m/sec at ambient chamber pressure and 72 m/sec at 1.34 MPa. At 4 mm Hg and atmospheric pressure, the spread angle of the spray at initial stage was much wider than at any other time during injection. At the highest chamber pressure, the spray angle was nearly constant throughout the injection. An interesting feature of the spray is seen for the low pressure case; surface waves of a constant spatial frequency appear to be a source of spray breakup. The fish-bone shaped structure of these surface waves are repeatable and believed to be a result of Kelvin-Helmholtz instabilities [15] where the initial perturbation is likely occurring in the nozzle. These waves are perhaps also observable in the atmospheric pressure condition, although they are apparently obscured or of such a short wavelength as to not be observable at the highest chamber pressure. Note that all of the velocity size data presented here were obtained for atmospheric pressure conditions. From these photographs, it is possible to discern ligaments of fluid and droplets. The spray itself does not appear to be completely opaque. However, at the high pressure conditions the spray appears to be much more dense, which has limited the accuracy of the data achievable with the PDPA. It is possible that under high temperature conditions, vaporization may make this spray somewhat less dense, and allow for a similar set of measurements as were obtained for the atmospheric pressure case.

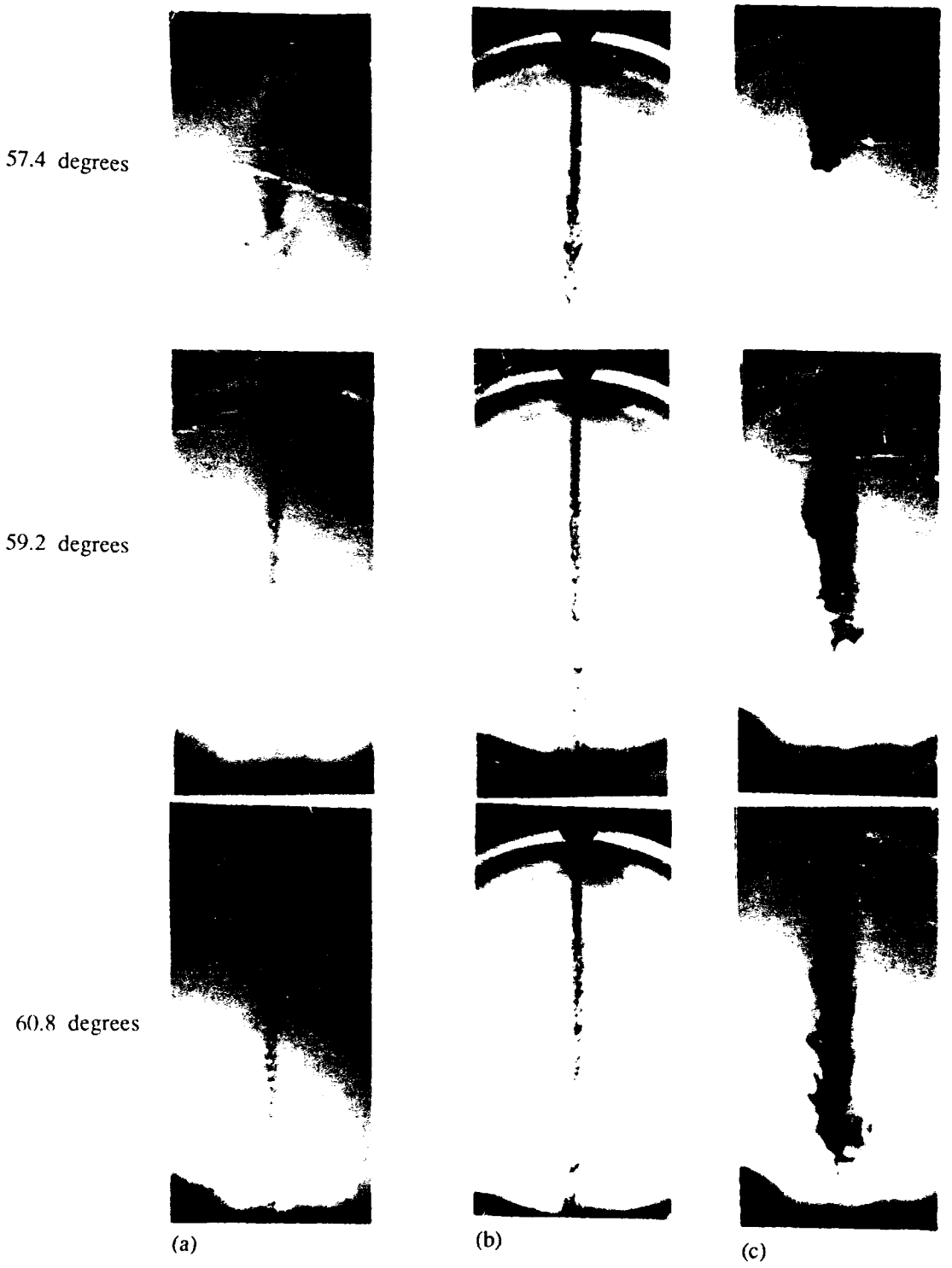


Fig 10. Single-shot spray photographs at 800 rpm and 19.5 mg per injection. Chamber pressure; (a) 4 mm Hg (b) Atmospheric pressure (c) 1.34 MPa with nitrogen

SUMMARY - From these measurements and observations of the spray from a transient diesel fuel injector:
1. The rate-of-injection and discharge coefficients rise rapidly as the needle opens to relatively constant values of 3.5 mg/cam degree and 0.72, respectively. The rate of change in these quantities is much greater during nozzle opening than during nozzle closing.
2. From measurements along the axis of the spray, a) the peak velocities are reduced as the axial distance from the nozzle is increased, b) close to the nozzle, the first injected droplets are apparently quickly overtaken by the droplets that follow them, c) the rate at which the velocity decreases after the end of injection is reduced as the axial distance from the nozzle is increased, d) the droplet diameter range is much larger nearer the nozzle, giving much larger values of d32 near the nozzle.
3. As the fuel quantity delivered is increased, the amount of time that the injection displays steady behavior increases.
4. Pump rotational speed has a strong effect on the behavior of the spray. For this injection system, the maximum velocity of the droplets is reduced at the 400 rpm speed, but similar at the higher speeds. For the 400 rpm condition, the behavior of the spray is never steady, as the velocity and droplet size distribution change throughout the duration of the spray.
5.Both drop velocity and diameter distributions show very strong dependence on the radial position in the spray. The largest droplets and peak velocities occur right on the axis of the spray. There is a continuous decrease in the magnitude of these quantities and the time at which they are affected by the transient injection as the radial coordinate is increased.
6. Gas-phase velocities show rapid acceleration right near the injector tip at the start of injection. Immediately after the end of injection, the gas surrounding the nozzle rapidly decelerates droplets near the nozzle, while further downstream, the entrained gas tends to cause the spray to stretch.
7. Short-exposure still photographs of the spray at three different ambient gas pressures showed that the spray angle was not constant during the injection at the two lowest pressure conditions. Further, surface waves were observed at these same two conditions which may be partly responsible for the observed breakup of the spray.

ACKNOWLEDGEMENTS - The authors wish to acknowledge Glenn Bower and Jeff Naber for their help in the spray photography. General Motors is acknowledged for the donation of the experimental injector used in this study. Support from Kia Motors Corporation for this study is acknowledged. Partial support for this work came from funding administered by the Army Research Office for the Engine Research Center.

REFERENCES

1. Heywood, J.B., Internal Combustion Engine Fundamentals, McGraw-Hill, 1988.

2. Arai, M., Tabata, M., Hiroyasu, H., and Shimizu, M., "Disintegrating Process and Spray Characterization of Fuel Jet Injected by a Diesel Nozzle," SAE Paper 840275, 1984.

3. Wu, K.J., "Atomizing Round Jets," Princeton University, Department of Aerospace Engineering, Ph.D. Thesis 1612-T, 1983.

4. Arai, M., Shimizu, M., and Hiroyasu, H., "Break-up Length and Spray Angle of High Speed Jet," ICLASS-85, London,1985.

5. Chehroudi, B., Chen, S.H., Bracco, F.V., and Onuma, Y., "On the Intact Core of Full-Cone Sprays," SAE Paper 850126, 1985.

6. Hiroyasu, H., Kadota, T., and Arai, M., "Supplementary Comments: Fuel Spray Characterization in Diesel Engine," Combustion Modeling in Reciprocating Engine, Plenum Press, 1980.

7. Wu, K.J., Su, C.C., Steinberger, R.L., Santavicca, D.A., and Bracco, F.V., "Measurement of the Spray angle of Atomizing Jets," Journal of Fluids Engineering, Vol. 105, pp. 406-413, 1983.

8. Yule, A.J., Mo, S.L., Tham, S.Y., and Aval, S.M., "Diesel Spray Structure," ICLASS-85, London, 1985.

9. Reitz, R.D., and Bracco, F.V., "On the Dependence of Spray Angle and Other Spray Parameters on Nozzle Design and Operating Conditions, " SAE Paper 790494, 1979.

10. Wu, K.J., Reitz, R.D., "Measurements of Drop Size at the Spray Edge near the Nozzle in Atomizing Liquid Jet," Phys. Fluids 29(4), April, 1986.

11. Reitz, R.D., "Atomization and Other Breakup Regimes of a Liquid Jets," Princeton University, Department of

Aerospace Engineering, PhD. Thesis, 1375-T, 1978.

12. Coghe, A., Gamma, F., Brunello, G., and Salmoiraghi, R., "LDV Analysis of Fuel Spray in a Diesel Engine Simulator," X task Leaders Meeting of the International Energy Agency, Amalfi, September, 1988.

13. Arcoumanis, C., Cossali, E., Paal, G., and Whitelaw, J.H., "Transient Characteristics of Single-Hole Diesel Sprays," SAE Paper 890314, 1989.

14. Reitz, R.D., and Diwakar, R., "Effect of Drop Breakup on Fuel Sprays," SAE Paper 860469, 1986.

15. O'Rourke, P.J., "Collective Drop Effects on Vaporizing Liquid Sprays," Princeton University, Department of Aerospace Engineering, PhD. Thesis 1532-7, 1981.

16. Faeth, G.M., "Mixing, Transport and Combustion in Sprays," Prog. Energy Combust. Sci. Vol. 13, 1987.

17. Bower, G., Chang, S.K., Corradini, M.L., El-Beshbeeshy, M., Martin, J.K., and Krueger, J., "Physical Mechanism for Atomization of a Jet Spray: A Comparison of Models and Experiments," SAE Paper 881318, 1988.

18. Reitz, R.D., and Diwakar, R., "Structure of High Pressure Fuel Sprays," SAE Paper 870598, 1987.

19. Reitz, R.D. and Bracco, F.V., "Mechanism of Atomization of a Liquid Jet," Phys. Fluid 25(10), October 1982.

20. Borman, G.L., "Reciprocating Engine Combustion Research Needs," SAE Paper 850398, 1985.

21. Switzer, G.L. and Jackson, T.A., "Investigation of Velocity and Turbulence Intensity Measurement Limitations of the Phase Doppler Particle Analyzer," 1988 Spring Technical Meeting, Central States Section, The Combustion Institute, May 2-3, 1988.

22. Kraemer, G. and Bachalo, W., "Evaluation of a Phase Doppler Particle Analyzer for Measuring Dense Sprays From a Gas Fuel Injector," AIAA-86-1532, 1986.

23. Jackson, A.A. and Samuelson, G.S., "Droplet Sizing Interferometry: A Comparison of the Visibility and Phase/Doppler Techniques," Applied Optics, 26(11), 1987.

24. Dodge, L.G., Rhodes, D.J., and Reitz, R., "Drop-size Measurement Techniques for Sprays: Comparison of Malvern Laser-Diffraction and Aerometrics Phase/Doppler," Applied Optics, 26(11), 1987.

25. McDonnell, V.G., Wood, C.P., Samuelson, G.S., "A Comparison of Spatially-Resolved Drop Size and Drop Velocity Measurements in an Isothermal Chamber and a Swirl-Stabilized Combustor," Twenty-First Symposium (International) on Combustion, The Combustion Institute, 1986.

26. Ghandhi, J.B. and Martin, J.K., "Errors Associated with Laser Doppler Velocimeter and Phase/Doppler Diameter Measurements in Combusting Flows," 1989 Spring Technical Meeting, Central States Section, The Combustion Institute, 1989.

27. Bower, G.R. and Foster, D.E., "Investigation of the Characteristics of a High Pressure Injector," SAE Paper 892101, 1989.